12th National Conference on Earthquake Engineering
Salt Lake City, Utah
27 June - 1 July 2022
Hosted by the Earthquake Engineering Research Institute

# Time-Dependent Seismic Hazard Assessment For a Case of Induced Seismicity in the United Kingdom

A.F. Hernandez[1], S. Drouet[2], P. Guéguen[3], B. Edwards[4], R. Secanell[2]

## ABSTRACT

The seismic hazard level at a site or a region can be estimated following a deterministic or probabilistic approach. The latter is the most widely used in several applications both in academia and industry. However, this methodology is based on the fact that all the events are independent of each other, and it is well known that the earthquake activity varies with time, especially in induced seismicity applications where the spatial and temporal distribution of events depends on the characteristics of the operation as well as the site where it takes place. This study addresses the problem of time-dependency focusing on a case study of induced seismicity in the United Kingdom where hydraulic fracturing operations were carried out to extract gas at the Preston New Road (PNR) site. The analysis was conducted per operational unit time (sleeve) obtaining exceedance rates which were computed using a ground motion prediction model for the site. The results suggest that the sleeve exceedance rates are related to the maximum magnitude, the number of events and the cumulative volume injected in each stage.

## Introduction

In the United Kingdom, induced seismicity is a subject that has been studied several years ago but only a few projects of this type were carried out in the last decade. One specific type of these projects is hydraulic fracture (HF) stimulation, which is widely used in the commercial production of hydrocarbons and in developing engineered geothermal systems worldwide (1,2). The HF is a technique to extract petroleum resources from impermeable host rocks through a high-pressure fluid injection causing fractures that result in induced earthquakes (3). In the UK, only three wells have been hydraulic fractured (HF) within the Carboniferous Bowland Shale formation, a reservoir with properties comparable to the major producing shale reservoir in North America (4–6). All of these three operational sites ended up in events felted by the population and created a controversy about this kind of activity in the country. The first well drilled was the Preese Hall well, stimulated in 2011 and generated a local magnitude of $M_L$ 2.3, which caused an intervention by the government leaving, as a result, the implementation of a traffic light system (TLS) to mitigate the risk and extended to other sites (Oil and Gas Authority (OGA), 2018). The effectiveness of this method is a subject that is still in the debate between the private and the academia (8–10). The idea behind the TLS is to minimize the number of events felt by the public and to avoid structural and/or non-structural damages. In 2018 two horizontal wells

[1] PhD Student, ISTerre, Université Grenoble Alpes, Grenoble, France (andres.hernandez@univ-grenoble-alpes.fr)
[2] Seismologist, Seismic Hazard Team, FUGRO France, Auriol, France
[3] Researcher, ISTerre, Université Grenoble Alpes, Grenoble, France
[4] Reader, School of Environmental Sciences, University of Liverpool, Liverpool, United Kingdom

Hernandez, A.F, Drouet, S., Guéguen, P., Edwards, B., Secanell, R. Time-dependent model for an induced seismicity case in the UK. *Proceedings of the 12th National Conference in Earthquake Engineering*, Earthquake Engineering Research Institute, Salt Lake City, UT. 2022.

at the Preston New Road site, approximately 4 km to the south of the Press Hall site, aimed to extract shale gas by HF and started operations with the eyes of the general public on it due to previous experience but it ended up in an event of $M_L$ 1.5 and the operations stopped. Later on, after a period of calm in 2019, the operations started again reaching an event of $M_L$ 2.9 leaving as a result of the indefinite interruption of the project until today. With all of this in mind, this document aims to study the seismicity variations in time for the HF at the Preston New Road site and introduce them into the estimation of the seismic hazard at the site.

## Data

The dataset used in this study corresponds to the shale gas extraction site in Preston New Road (PNR), North West England, where hydraulic fracturing (HF) operations were carried out in two different periods, between 15 October to 17 December 2018 (hereinafter PNR-1z), and later on between 15 August to 02 October of 2019 (hereinafter PNR-2) (11,12). To monitor the operation an array of sensors, including broadband seismometers and geophones were installed at the surface and downhole of the site, for the company in charge of the operation, Cuadrilla Resources Ltd (CRL), in collaboration with the British Geological Survey (BGS) and the University of Liverpool (8). During the first period of operation (PNR-1z), the events recorded were between $-0.8 \leq M_L \leq 1.5$ and between $-1.7 \leq M_L \leq 2.9$ for the second period (PNR-2), crossing several times all the flags of the TLS system imposed in the UK and having, as a result, the temporary and permanent suspension of the operation at the site. Both wells (PNR-1z and PNR-2) ran through the natural gas-bearing Carboniferous formation of the Lower Bowland shale at a depth of approximately 2.3 km (5). In the case of the PNR-1z well, a sliding-sleeve completion method was used, with 41 individual sleeves numbered ascending from toe to the heel of the well, and a hydraulic fracture plan up to 765 m3 of fluid per sleeve was set (13). However, a total number of 16 sleeves were hydraulically fractured with a total of about 4,600 m3 of fluid injected and an average volume for each fracture of 234 m3 with a maximum of 431 m3 (14). On the other hand, the PNR-2 well followed the same sleeve method performed up to 7 possible hydraulic fracture stages. Fig 1 presents the spatial and temporal distribution of both datasets, PNR-1z, and PNR-2, with a scheme color according to each sleeve for both cases.

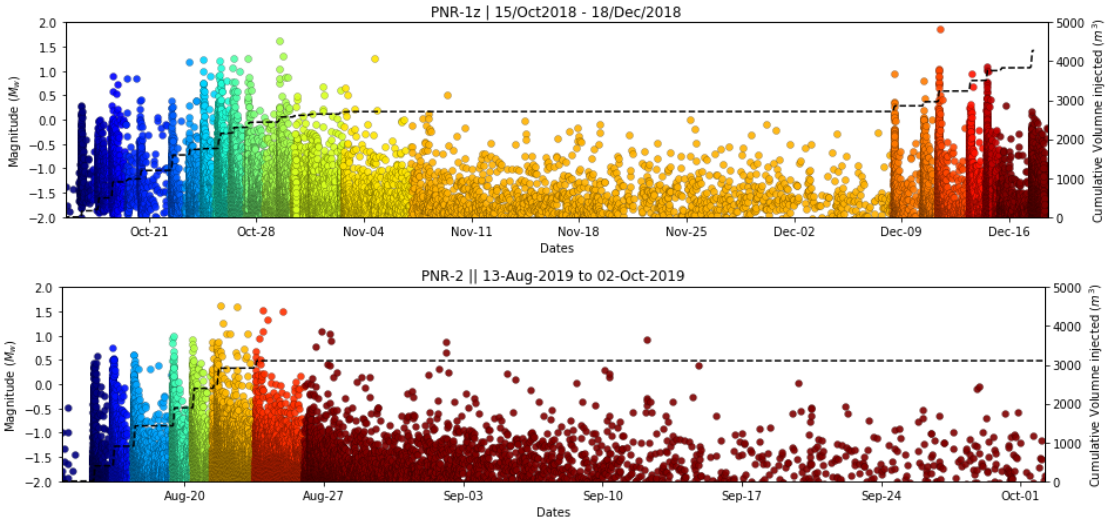


Figure 1. Temporal distribution of the datasets PNR-1z and PNR-2. Dotted line: cumulative volume injected ($m^3$). Top: PNR-1z. Bottom: PNR-2.

## Seismic Hazard Calculation

To estimate the seismic hazard level for the induced earthquakes at the site, we studied both datasets (PNR-1z and PNR-2) independently using the unit-time per *sleeve* according to the injection plan; it is important to mention that each sleeve represents the different steps in the operation of the HF process at the site. The seismic parameters (*a* and *b* values) were obtained following the Gutenberg-Richter (GR) distribution (15).

$$\log(N) = a - bm \quad (1)$$

where $N$ is the number of earthquakes with a magnitude greater than magnitude, $m$. The $a$-value indicates the number of earthquakes per unit time duration, while the $b$-value represents the ratio of small and large magnitude events. The maximum magnitude ($M_{max}$) used for all the sleeves was set to 4.5, which is the minimum tectonic magnitude presented in the seismic hazard model for the area. Fig. 2 shows the magnitude-frequency distribution (MFD) per sleeve with the respective information of seismic parameters, days, and the number of events registered. For illustration purposes, only 9 sleeves are presented for the PNR-1z dataset, which corresponds with the major number of events.

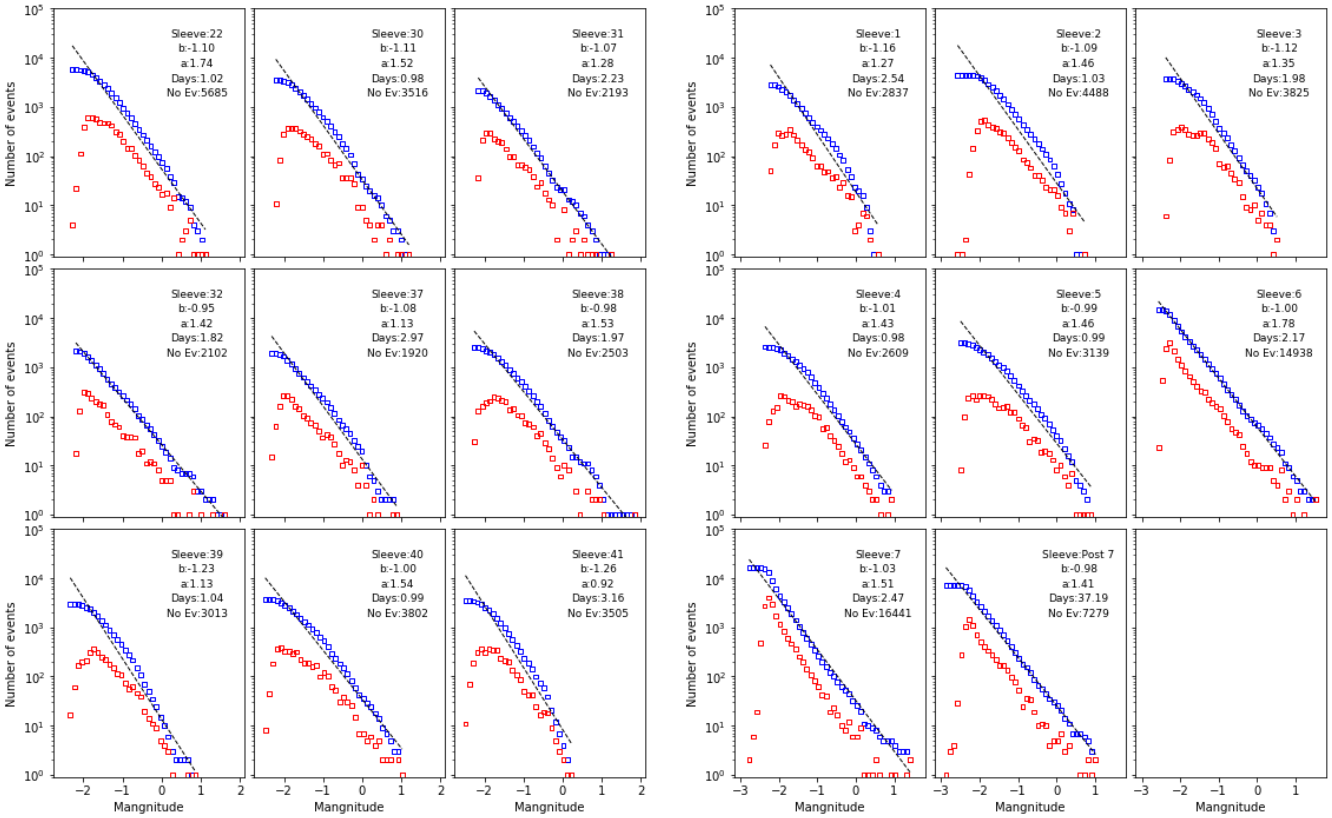


Figure 2. Magnitude-Frequency distributions (MFD) per sleeve. Left: PNR-1z dataset, sleeves 22, 30-32, 37-41. Right: PNR-2 dataset, sleeves 1-7 and Post 7. Blue squares: Cumulative. Red squares: Incremental.

Once the seismic parameters per sleeve are obtained we perform the probabilistic seismic hazard assessment (16,17) at the site as follows, 1) selecting the ground-motion model (GMM) proposed by (18), which was estimated for the same site based on the GMMs by (19,20); 2) modeling the seismic source as a point source for each sleeve with the fault parameters (strike, dip, and rake) estimated for the site proposed by (21,22); 3) computing the seismic hazard curves at the site using the OpenQuake Engine (23,24).

## Results

The seismic hazard curves using the GMM by (18) are presented in Fig 3, following the same scheme color in Fig. 1 for both datasets, PNR-1z, and PNR-2. We decided to perform the analysis of the exceedance rates per each sleeve (hereinafter *sleeve exceedance rates*), taking into account that we have all the seismicity per that operational unit time. The sleeve exceedance rates were computed from two perspectives, 1) *independent sleeve*, which means that each curve represents the exceedance rates during the sleeve time, which is not always the same, and 2) *consecutive sleeve*, in which each curve represents the exceedance rates from all the previous

sleeves, by adding the previous sleeves but considering the all the duration. The results show a dependency between the sleeve exceedance rates and the magnitude per each sleeve, the greater the magnitude in the sleeve, the higher the exceedance rates. Observing the results by independent sleeve the last state for both datasets (Hiatus and 8 = Post 7) has the lowest rates and the highest ones usually are the sleeves with higher magnitudes. In terms of consecutive sleeves, the highest exceedance rates for dataset PNR-1z are for sleeves 38 and 39, but sleeves 18, 22, 30-32, 37, and 40 have high exceedance rates, while for the dataset PNR-2 the higher rates are in the sleeves 4-7. Finally, there is a strong impact of the cumulative injected volume (see dotted lines in Fig. 1) in the exceedance rates. In most cases, the sleeve with higher rates occurs when the volume injected increases.

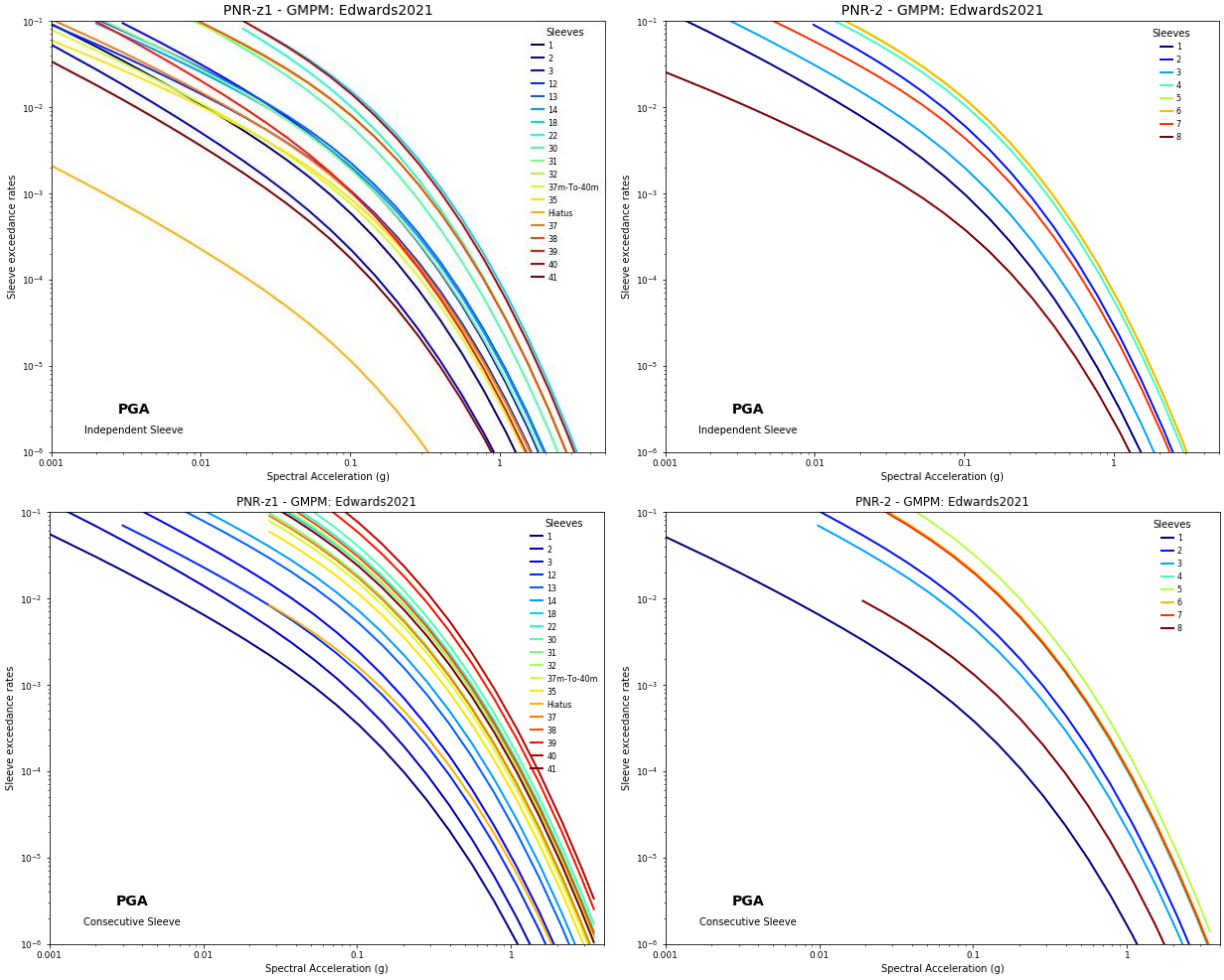


Figure 3. Seismic hazard curves for PGA using the GMM by (18). Color scheme same as Fig. 1. Top: Independent sleeve exceedance rates. Bottom: Consecutive sleeve exceedance rates (adding the previous sleeves). Left: PNR-1z dataset. Right: PNR-2 dataset.

## Conclusions

In this study, we compute the exceedance rates for an induced seismicity case in the United Kingdom, where hydraulic fracturing operations were carried out to extract gas at the Preston New Road (PNR) site. The aim was to include the variation in time of the seismicity and to do so we analyzed both datasets (PNR-1z and PNR-2) per sleeve unit time, which is attached to an operational decision. The results showed that the sleeve exceedance rates either using an independent or consecutive sleeve calculation approach, are directly related to the maximum magnitude, the number of the events, and the cumulative volume injected of the sleeve. The evolution of the exceedance rates per sleeve provides an insight into how the seismic intensity levels at the site were varying during the hydraulic fracturing operations at the site.

## Acknowledgments

This research has been funded by the EU Horizon 2020 program under Grant Agreement Number 813137, ITN-MSCA New challenges for Urban Engineering Seismology (URBASIS) project.

## References

1. Igonin N, Verdon J, Kendall J-M, Eaton D. The importance of pre-existing fracture networks for fault reactivation during hydraulic fracturing. Earth Sp Sci Open Arch. 2019;(May).
2. Langenbruch C, Ellsworth WL, Woo JU, Wald DJ. Value at Induced Risk: Injection-Induced Seismic Risk From Low-Probability, High-Impact Events. Geophys Res Lett. 2020;47(2).
3. Schultz R, Skoumal RJ, Brudzinski MR, Eaton D, Baptie B, Ellsworth W. Hydraulic fracturing-induced seismicity. Rev Geophys. 2020;58(3):1–43.
4. Kettlety T, Verdon JP, Butcher A, Hampson M, Craddock L. High-Resolution Imaging of the ML 2.9 August 2019 Earthquake in Lancashire, United Kingdom, Induced by Hydraulic Fracturing during Preston New Road PNR-2 Operations. Seismol Res Lett. 2021;92(1):151–69.
5. Clarke H, Turner P, Bustin RM, Riley N, Besly B. Shale gas resources of the Bowland Basin, NW England: a holistic study. Pet Geosci [Internet]. 2018 Aug;24(3):287–322. Available from: http://pg.lyellcollection.org/lookup/doi/10.1144/petgeo2017-066
6. Verdon JP. Significance for secure CO2 storage of earthquakes induced by fluid injection. Environ Res Lett. 2014;9(6).
7. Oil and Gas Authority. Consolidated Onshore Guidance, Version 2.2 [Internet]. 2018. Available from: https://www.ogauthority.co.uk/media/4959/29112017_consolidated-onshore-guidance-compendium_vfinal-002.pdf
8. Clarke H, Verdon JP, Kettlety T, Baird AF, Kendall JM. Real-time imaging, forecasting, and management of human-induced seismicity at Preston new road, Lancashire, England. Seismol Res Lett. 2019;90(5):1902–15.
9. Verdon JP, Bommer JJ. Green, yellow, red, or out of the blue? An assessment of Traffic Light Schemes to mitigate the impact of hydraulic fracturing-induced seismicity. J Seismol. 2021;25(1):301–26.
10. Baisch S, Koch C, Muntendam-Bos A. Traffic light systems: To what extent can induced seismicity be controlled? Seismol Res Lett. 2019;90(3):1145–54.
11. Cuadrilla Resources. Preston New Road-1z HFP report. Tech Rept PNR1z-HFP-Rept-001 [Internet]. 2019;1–25. Available from: https://www.ogauthority.co.uk/media/5845/pnr-1z-hfp-report.pdf
12. Cuadrilla Resources. Hydraulic fracture plan PNR 2. Tech Rept CORP-HSE-RPT-003 [Internet]. 2019;1–21. Available from: https://cuadrillaresources.com/site/preston-new-road/
13. Baptie B, Luckett R, Butcher A, Werner MJ. Robust relationships for magnitude conversion of PNR seismicity catalogues. Br Geol Surv Open Rep [Internet]. 2020;OR/20/042:32pp. Available from: https://www.ogauthority.co.uk/exploration-production/onshore/onshore-reports-and-data/preston-new-road-well-pnr2-data-studies/
14. Mancini S, Werner MJ, Segou M, Baptie B. Probabilistic Forecasting of Hydraulic Fracturing-Induced Seismicity Using an Injection-Rate Driven ETAS Model. Seismol Res Lett [Internet]. 2021 May 19; Available from: https://pubs.geoscienceworld.org/ssa/srl/article/598748/Probabilistic-Forecasting-of-Hydraulic-Fracturing
15. Gutenberg R, Richter CF. Frequency of earthquakes in California. Bull Seismol Soc Ameroca. 1954;34:185–8.
16. Cornell CA. Engineering seismic risk analysis. Bull Seismol Soc Am. 1968;58(5):1583–606.
17. Esteva L. Regionalizacion sismica de la Republica Mexicana. Rev Soc Mex Ing Sismica. 1963;1:31–5.
18. Edwards B, Crowley H, Pinho R, Bommer JJ. Seismic Hazard and Risk Due to Induced Earthquakes at a Shale Gas Site. Bull Seismol Soc Am. 2021;1–23.
19. Atkinson GM. Ground-Motion Prediction Equation for Small-to-Moderate Events at Short Hypocentral Distances, with Application to Induced-Seismicity Hazards. Bull Seismol Soc Am [Internet]. 2015 Apr;105(2A):981–92. Available from: https://pubs.geoscienceworld.org/bssa/article/105/2A/981-992/332710
20. Douglas J, Edwards B, Convertito V, Sharma N, Tramelli A, Kraaijpoel D, et al. Predicting Ground Motion from Induced Earthquakes in Geothermal Areas. Bull Seismol Soc Am [Internet]. 2013 Jun 1;103(3):1875–97. Available from: https://pubs.geoscienceworld.org/bssa/article/103/3/1875-1897/349891

21. Kettlety T, Verdon JP. Fault Triggering Mechanisms for Hydraulic Fracturing-Induced Seismicity From the Preston New Road, UK Case Study. Front Earth Sci. 2021;9(May):1–15.

22. Clarke H, Soroush H, Wood T. Preston new road: The role of geomechanics in successful drilling of the UK's first horizontal shale gas well. Soc Pet Eng - SPE Eur Featur 81st EAGE Conf Exhib 2019. 2019;1–23.

23. Silva V, Crowley H, Pagani M, Monelli D, Pinho R. Development of the OpenQuake engine, the Global Earthquake Model's open-source software for seismic risk assessment. Nat Hazards. 2014;72(3):1409–27.

24. Pagani M, Monelli D, Weatherill G, Danciu L, Crowley H, Silva V, et al. OpenQuake Engine: An Open Hazard (and Risk) Software for the Global Earthquake Model. Seismol Res Lett [Internet]. 2014 May 1;85(3):692–702. Available from: https://pubs.geoscienceworld.org/srl/article/85/3/692-702/315386